ELSEVIER

Contents lists available at ScienceDirect

Energy Reports

journal homepage: www.elsevier.com/locate/egyr



Research paper

Multi-effect distillation for water desalination in an offshore PEM electrolyser system

M. Haqiqi ^{a,b}, S. Dussi ^a, J. Garcia-Navarro ^{a,*}



^b Utrecht University, Copernicus Institute of Sustainable Development, Utrecht 3508TC, the Netherlands

ARTICLE INFO

Keywords:
Offshore Green Hydrogen
PEM Electrolyzer
Multi-Effect Distillation (MED)
Desalination
Waste Heat Utilization
Renewable Energy Systems
Energy Integration

ABSTRACT

We study the integration of Multi-Effect Distillation (MED) desalination systems with Proton Exchange Membrane electrolysers (PEMEL) for large-scale offshore hydrogen production. The focus is on utilising the waste heat generated by PEMEL to drive the MED process. The developed quasi-steady-state model shows that MED can consistently meet the water demands of a 1 GW PEM electrolyser, except for electrolyser input power below 5 % of the nominal load. We find that at full load, a large part of the excess heat (up to 94.12 MW) remains uncollected, highlighting a need for further thermal management solutions. For the optimal MED design, we calculate a Gain Output Ratio (GOR) of 3.69, Specific Heat Consumption (SHC) of 631.54 kJ/kg, and a Specific Heat Transfer Area (area per kg/s distillate) of 155.12 $m^2/kg/s$. For this configuration, MED is estimated to occupy a footprint of around 130 m^2 in a horizontal arrangement, while the 1 GW PEMEL occupies approximately 12000 m^2 .

1. Introduction

The transition towards renewable energy sources has become a crucial global directive to combat climate change and achieve a sustainable future. The move towards clean energy is supported by international agreements, such as the Paris Agreement, where countries have committed to reducing their greenhouse gas emissions (Erickson and Brase, 2019). Renewable energy is an essential part of this effort since it offers a practical solution to reduce one of the primary sources of emissions, namely energy production. Aligned with the Paris Agreement, "The European Green Deal" set binding targets of 55 % fewer emissions by 2030 and reaching carbon neutrality by 2050 were published by the European Commission in 2019 (European Commission, 2019). As a member state, the Netherlands not only initially committed (The Government of Netherlands, 2019) to a 49 % reduction by 2030, but has revised it to a 55 % reduction by 2030. Furthermore, the Netherlands announced in 2022 the ambitious goal of increasing its offshore wind targets from 11 to 21 gigawatts (GW) by 2030 and aiming for 70 GW capacity by 2050 (Netherlands Enterprise Agency, 2021). Consequently, cost-effective and environmentally friendly ways of turning the Netherlands' vast wind resource into dispatchable power are urgently required.

The intermittent nature of wind generation, coupled with grid congestion constraints, promotes the opportunity to transition towards green hydrogen as it can serve as a storage or energy carrier within the future power system (Van der Welle and De Joode, 2011; Ghaemi et al., 2023; Barbir, 2005). Additionally, because of the lower costs of transporting hydrogen molecules to shore through pipelines compared with electrons through cables, anddue to the potential savings by reusing current oil and gas infrastructure in the North Sea, the ongoing development of offshore wind projects offers a strategic opportunity for integrating green hydrogen to mitigate costs (Siachos, 2022; Brosschot, 2022; Amos, 1999). As such, the synergetic relationship between offshore wind projects and green hydrogen integration emerges as a forward-looking approach to address intermittency concerns and economic efficiency in the evolving energy landscape in the decarbonised power system. Accordingly, the Dutch government has unveiled plans to establish the world's largest offshore green hydrogen production plant, installing 500 Megawatts (MW) capacity by 2031 (Buljan, n.d). This groundbreaking initiative will feature the deployment of the first large-scale offshore electrolysers. This rise in electrolyser capacity poses

Abbreviations: BF, Backward Feed; CEDI, Continuous Electro Deionisation; FF, Forward Feed; IX, Ion Exchange; MED, Multi-Effect Distillation; MSF, Multi-Stage Flash; MVC, Mechanical Vapour Compression; PCF, Parallel/Cross Feed; PEM, Proton Exchange Membrane; PEMEL, Proton Exchange Membrane Electrolyser; PF, Parallel Feed; TDS, Total Dissolved Solids; TEMA, Tubular Exchanger Manufacturers Association; TVC, Thermal Vapour Compression.

E-mail address: julio.garcianavarro@tno.nl (J. Garcia-Navarro).

https://doi.org/10.1016/j.egyr.2025.07.031

Received 14 January 2025; Received in revised form 18 June 2025; Accepted 7 July 2025 Available online 26 July 2025

^{*} Corresponding author.

Nomenclature		P_{sat}	Saturated pressure (mbar)
		P_{sat}	Saturated pressure (mbar)
A_c	Heat transfer area of condenser (m ²)	P_{v}	Vacuum pressure (mbar)
$\Lambda_{ m ei}$	Heat transfer area of i th effect (m ²)	Q_{i}	Heat transfer in effect (kW)
B_i	Brine flowrate (kg/s)	Q_{waste}	Waste heat (kW)
3PE	Boiling Point Elevation (°C)	S_a	Specific heat transfer area (m ² / (kg/s))
$\mathcal{L}_{\mathbf{p}}$	Specific heat capacity (kJ/kg.°C)	SHC	Specific Heat Consumption (kJ/kg)
$\hat{D_i}$	Distillate flowrate (kg/s)	T_{bn}	Last brine temperature (°C)
Einput	Total electrical energy input	T_c	Critical temperature (°C)
reaction	Reaction energy	T_{cw}	MED cooling water temperature (°C)
\vec{s}_{i}	Feed flowrate (kg/s)	$T_{\mathbf{f}}$	Feed water temperature (°C)
GOR	Gain Output Ratio	T_{i}	Temperature of brine or effect (°C)
$\mathbf{1_f}$	Saturated water enthalpy (kJ/kg)	T_{PEM}	Stack temperature (°C)
1_{fg}	Latent heat of evaporation (kJ/kg)	T_s	Steam temperature (°C)
1 _g	Saturated steam enthalpy (kJ/kg)	T_{sat}	Saturation temperature (°C)
Η̈́ΗV	Higher Heating Value (kJ/kg)	T_{sw}	Seawater temperature (°C)
LMTD	Log Mean Temperature Difference	T_{vi}	Vapour temperature entering the effect
n_{H2}	Mass of hydrogen produced (kg/s)	$ m U_{ei}$	Heat transfer coefficient of evaporator (kW/m ² .K)
n_s	Steam mass flowrate (kg/s)	U_c	Heat transfer coefficient of condenser (kW/m ² .K)
1	Number of effects	V_{i}	Vapour flowrate (kg/s)
atm	Atmospheric pressure (mbar)	X_b	Brine salinity (g/kg)
P _C	Critical pressure (mbar)	X_{f}	Feedwater salinity (g/kg)

many challenges, including the increased pure water demand and the management of the waste heat released from the electrochemical process. This scenario is further complicated by the unfavourable impacts of thermal pollution on marine ecosystems, as highlighted by Kennedy (Kennedy, 2004), which shows the importance of environmentally responsible waste heat management. In fact, the waste heat produced by Proton Exchange Membrane (PEM) electrolyser could go up to 70-80°C (Joris, 2019; Buttler and Spliethoff, 2018; van der Roest et al., 2023). Innovative solutions are therefore needed to prevent the ecological risks associated with the disposal of this waste heat into the seawater (Joris, 2019).

A growing body of work therefore explores hybrid wind-hydrogen systems, yet the handling of the electrolyser's large, low-grade heat stream remains largely overlooked. This oversight becomes critical offshore, where conventional heat-rejection options are both costly and ecologically sensitive. One proposed approach is to leverage this excess heat for water desalination using Multi-Effect Distillation (MED) (Ellersdorfer et al., 2023). This method harmonises well with PEM electrolysers because MED requires low-temperature heat, as it can utilise the low-grade waste heat of PEM electrolysers. Conversely, PEM electrolysers need water as an essential input for their electrochemical process. Therefore, incorporating waste heat from electrolysers into multi-effect desalination has the potential to simultaneously enhance the overall system resource management for offshore hydrogen production and mitigate environmental concerns associated with releasing heated water into the ocean. Additionally, it is important to recognise the common difficulties encountered with the most widely used desalination method desalination method, namely Reverse Osmosis (RO), such as membrane fouling (Wenten and Khoiruddin, 2016). This can cause a decrease in flux, an increase in operational pressures, and higher pre-treatment and maintenance costs (Jamaly et al., 2014; Qasim et al., 2019). Moreover, RO processes require a significant amount of electricity, particularly to overcome osmotic pressures, compared to other desalination processes. These shortcomings associated with the RO method make the investigation of MED desalination even more intriguing.

Against this backdrop, researchers have tested several ways to recycle industrial waste heat in MED and related desalination schemes. Recent advancements in integrating renewable energy and industrial waste heat with MED have demonstrated various innovative approaches

to improve the thermodynamic and economic performance of the systems. For example, Liponi and colleagues (Liponi et al., 2020) explored new configurations for small-scale MED systems that better exploit low-temperature heat sources. By enhancing heat recovery, configurations implementing seawater preheating could increase the efficiency by up to 10 %, making these solutions particularly cost-effective when thermal energy costs become relevant (Liponi et al., 2020). Building on the concept of thermal efficiency, Zhao et al. (Zhao et al., 2011). conducted theoretical analyses focusing on MED desalination for high-salinity wastewater. Their work emphasised the importance of optimising the number of effects to balance lower costs with increased distillate production, highlighting the critical role of feed steam temperature and evaporator conditions in enhancing system efficiency (Zhao et al., 2011). Further emphasising the importance of energy source optimisation, Khalilzadeh and Hossein Nezhad (Khalilzadeh and Hossein Nezhad, 2018) investigated the use of waste heat from high-capacity wind turbines to provide the necessary steam for MED desalination. Their analysis revealed that such integration could provide sufficient potable water for a significant population (Khalilzadeh and Hossein Nezhad, 2018). Wang et al. (Wang et al., 2011). highlighted the advantages of low-grade heat-driven MED technologies, particularly in terms of minimising carbon dioxide emissions. In line with efforts to enhance water recovery and reduce environmental impact, Bamufleh et al (Bamufleh et al., 2017). introduced an optimisation approach for integrating MED with membrane distillation (MD) to increase freshwater recovery and decrease brine disposal. This integrated approach also proposed thermal coupling with industrial processes to leverage excess heat, presenting a compelling case for the cooperation between desalination systems and industrial energy efficiency (Bamufleh et al., 2017).

Aligned with advancements demonstrated in these recent studies, integrating MED with electrolyser systems for (offshore) green hydrogen production presents a novel avenue for sustainable water use. The technical aspects of such integration, including heat transfer mechanisms, system design, and operational parameters, present an attractive area for investigation. Factors such as the required heat transfer area, footprint area, and the optimal design of integrated systems are crucial considerations that need to be addressed to assess the viability and operability of this innovative approach. To date, however, no study has combined PEM-electrolyser waste-heat recovery with dynamic, offshore

MED operation.

This study makes three novel contributions:

- Waste-heat utilisation: We develop the first "zero-effect" MED concept that taps the 80°C cooling loop of a 1 GW offshore PEM electrolyser, turning a disposal loss into process steam.
- Dynamic, offshore-realistic operation: Using hour-by-hour Dutch wind data, we verify that the coupled MED can continuously satisfy electrolyser water demand, an operating regime untested in previous steady-state studies.
- Platform-level integration: We size heat-exchange area, footprint, and brine-temperature rise to prove the layout is feasible and that thermal pollution is cut, addressing an environmental gap flagged in earlier work.

The goal of this document is to assess the feasibility of integrating large-scale PEM electrolysers with MED seawater desalination in the North Sea. Firstly, the design characteristics and limitations of such integration will be examined, including a comparison between MED systems and conventional desalination methods when coupled with PEM electrolysers, as well as technical requirements and the potential impact on the marine ecosystem due to changes in brine temperature and salinity. Secondly, by developing a quasi-steady state model for MED desalination, operational conditions and challenges will be assessed. This model uses wind data from Dutch offshore wind generation to determine if the operational MED can fulfil the electrolyser water demand on an hourly basis. By providing a comprehensive understanding of the design specifications, technical challenges, and potential benefits associated with this approach, this study ultimately contributes to the sustainable and efficient offshore production of green hydrogen.

2. Review

Desalination is a critical technology for producing fresh water from saline sources, especially in regions where fresh water is scarce. The global desalination capacity is significant, with recent figures indicating a capacity of 38 billion cubic meters per year, consuming around 75 TWh of energy, primarily from fossil fuels (Elsaid et al., 2020). This highlights the extensive use of desalination technologies and their

energy-intensive nature. It is useful to build a comparison between the most common types of desalination technologies. As shown in Fig. 1.a, MED is a thermal process that uses multiple stages (or effects) where seawater is heated and evaporated, and the steam is condensed to produce fresh water. This process is particularly energy-efficient compared to the Single-effect Distillation thermal desalination method because it utilises the latent heat of vaporisation in multiple stages (Brogioli et al., 2018). The market share of operational desalination technologies (depicted in Fig. 1.b) shows a diversified approach, with membrane-based technologies, namely RO (68.7 %) and thermal technologies like MED (17.6 %) and Multi-Stage Flash (MSF) (6.9 %) being widely used (Curto et al., 2021). It is good to mention that Seawater desalination accounts for approximately 61 % of the global desalination capacity, indicating a significant reliance on oceanic water sources (Jones et al., 2019).

Different technologies are utilised globally, tailored to specific geographic and economic conditions. RO is the most prevalent technology and is predominantly used in Europe and other coastal regions due to its lower energy consumption compared to thermal methods (Greenlee et al., 2009; Fritzmann et al., 2007). MSF distillation is widely used in the Middle East and Gulf countries (Ismail, 1998; Mazzotti et al., 2000), where it accounted for over 44.6 % of regional installations in 2017 (Moossa et al., 2022). This method is favoured for its large-scale water production capabilities and the fact that fossil fuels, which are abundant and cheaper in these regions, are used to power these plants. Given the arid climate and limited freshwater resources in the Persian Gulf, the water demand is critical, making thermal desalination technologies particularly suitable. MED is less energy-intensive than MSF and is commonly used in the Middle East and North Africa, often in conjunction with renewable energy sources (Curto et al., 2021). Solar desalination is emerging as a sustainable alternative, particularly in regions with high solar irradiation, such as parts of Africa, the Middle East, India, and China. Additionally, hybrid plants that combine various desalination technologies, such as RO with thermal processes, are increasingly being used to enhance efficiency and reduce costs (Hammond, 1996).

According to the existing literature and industrial brochures, a comparison of the most common desalination technologies based on technological, economic, and environmental aspects is reported in

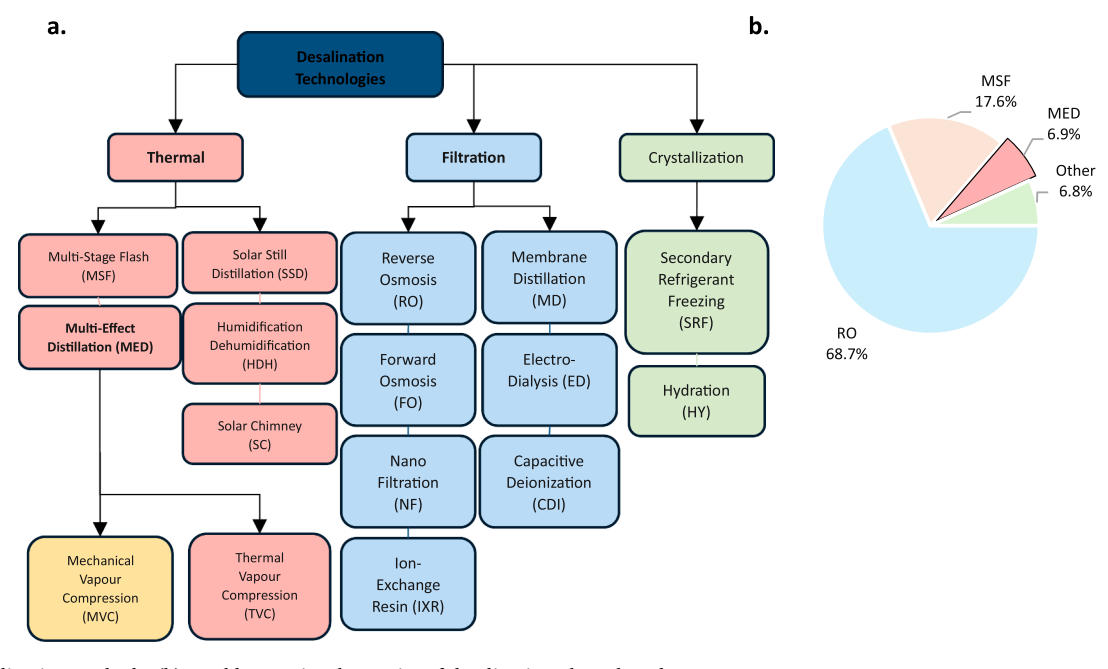


Fig. 1. (a) Desalination methods. (b) World operational capacity of desalination plants based on types. (a) Reproduced from the information of Curto et al. (2021). (b) Reproduced from data in Jones et al. (2019).

Table 1
Technological, economic, and environmental benefits and drawbacks associated with different desalination technologies. Comparison based on the literature (Ellersdorfer et al., 2023; Elsaid et al., 2020; Curto et al., 2021; Fritzmann et al., 2007; Jiang et al., 2017; Al-Shammiri and Safar, 1999; Al-Mutaz, 1996; Swiss, 2024; Veolia, 2014; Ihm et al., 2016; Mezher et al., 2011; Khawaji et al., 2008; Raluy et al., 2006; Al-Sahali and Ettouney, 2007).

Criteria / Category	RO	MSF	MED	References
Electricity Consumption (kWh/m³)	Moderate to high (3.3–5.0)	Moderate (2.2–5)	Low (1.0–1.4)	(Ellersdorfer et al., 2023; Curto et al., 2021; Swiss, 2024; Veolia, 2014; Ihm et al., 2016)
Possible Unit Size (kg/s)	Large (up to 580)	Very large (up to 700)	Moderate (55 up to 290 or 790 with TVC)	
Achievable GOR	Not applicable	High (10-14)	Moderate (8–10)	
Number of Effects	Not applicable	Up to 30	Up to 25	
Outlet Water Quality (ppm)	Low (40-400)	Very high (<5)	Very high (<5)	
Pretreatment Requirement	High	Low	Low	
Maintenance Requirements	High	High	Low	
Spare Parts Requirement	High (Membranes)	High	Low	
Heat Transfer Area	Not applicable	High	Low	
Failure due to Corrosion	High	High	Low	
Periodic Cleaning (months)	Moderate (3–12)	Frequent (3–6)	Infrequent (18–24)	
Operation Complexity	High	Moderate	Low	
Plan Life (years)	Low (12-15)	High (25-30)	High (25–30)	
Capacity Factor (%)	Moderate (92-95)	High (96-98)	High (96–98)	
Chemicals needed	Coagulant (20 mg/l)	Coagulant (20 mg/	Depends on operating conditions,	
during operation	Flocculant (0.5 mg/l)	1)	but expected to be similar to MED	
	Biocide (1 mg/l)	Flocculant	Coagulant (20 mg/l)	
	Antiscalant (2 mg/l)	(0.5 mg/l) Antiscalant (2 mg/l)	Flocculant (0.5 mg/l) Antiscalant (2 mg/l)	
Technological	Modular, scalable,	High capacity,	Long lifespan, less affected by	
Benefits	adaptable	water quality	feedwater quality, low energy consumption, water quality	
Technological Drawbacks	Membrane fouling, high maintenance	High energy demand, scaling issues	Complexity, higher energy consumption, scaling	(Curto et al., 2021; Fritzmann et al., 2007; Jiang et al., 2017; Al-Shammiri and Safar, 1999; Swiss, 2024; Mezher et al., 2011; Khawaji et al., 2008; Raluy et al., 2006; Al-Sahali and Ettouney,
Economic Benefits	Lower energy consumption than MSF	Economies of scale reduce costs	Cost-effective with low-grade waste heat	2007)
Economic Drawbacks	and MED High maintenance costs	Highest capital	Higher capital than RO	(Curto et al., 2021; Jones et al., 2019; Al-Mutaz, 1996; Mezher
		costs	-	et al., 2011; Raluy et al., 2006)
Environmental	Lower energy	Uses waste heat	Lower thermal energy requirement,	
Benefits	requirements, reduced emissions	effectively	reduced environmental impact	
Environmental Drawbacks	Brine disposal challenges	High thermal pollution, brine disposal	Thermal pollution and brine disposal	(Elsaid et al., 2020; Curto et al., 2021; Ahmed et al., 2001; Mezher et al., 2011; Raluy et al., 2006)

Table 1. RO is susceptible to membrane biofouling due to organic and biological matter deposition. This fouling not only necessitates frequent chemical cleaning but also shortens the lifespan of the RO membranes. The polymeric nature of these membranes makes them prone to degradation over time, particularly under harsh operational conditions in seawater desalination. In contrast, MED plants have a longer operational lifespan due to their robust thermal-based process, which is less affected by the feedwater quality and does not involve polymeric membranes susceptible to biofouling (Jiang et al., 2017). MED systems, despite their advantages, face several operational and economic challenges. The complexity of MED systems, which involve multiple stages of heating, can lead to higher capital costs compared to simpler desalination technologies like RO (Golkar et al., 2017; Kesieme et al., 2013). Additionally, MED plants are susceptible to scaling and fouling, decreasing heat transfer efficiency and necessitating frequent maintenance and cleaning, though to a lesser extent than RO systems. Furthermore, the reliance on thermal energy means that MED plants are most cost-effective when integrated with a source of low-cost waste heat or when energy prices are favourable. In the absence of such conditions, the operational costs of MED can be higher compared to other desalination technologies

(Elsaid et al., 2020; Do Thi et al., 2021). Furthermore, the lower energy consumption and reduced heat transfer area required per kg of water produced by MED systems contribute to their economic viability, making them competitive with MSF processes in terms of technical and financial performance (Al-Shammiri and Safar, 1999).

However, it is important to recognise that capital, operational costs, and technical performance of desalination technologies' can greatly depend on the specific situation, including plant scale, geographic location, available energy sources, and technological advancements. In addition, brine disposal methods are also key to assessing the environmental issues associated with different technologies and comparing them. For brine management, coastal areas often discharge brine into the sea, whereas inland regions utilise methods like lined evaporation ponds or advanced treatment processes (Ahmed et al., 2001). Thermal desalination adds another environmental concern to the system on top of brine salinity: the heat available in the brine. This makes brine disposal even more challenging, especially in offshore configurations, where environmental regulations could limit the brine disposal temperature.

Based on the data of Table 1, MED and MSF produce freshwater with salinity below 5 ppm. Although both technologies provide higher-

quality water than RO, further purification is still required, because this is still insufficient to operate PEMEL as it requires high-purity ASTM D1193-06 water (Inc, 2021). The ASTM D1193-06 standard establishes a maximum water conductivity of 0.056 5 $\mu S/cm$ (25°C) for Type I (laboratory water quality) water, (Atlas High Purity Solutions team team, 2019), which has been adopted by several PEM electrolyser original equipment manufacturers as the minimum water quality required (Inc., 2021). Using a 0.5 empirical factor to convert conductivity (in $\mu S/cm$) to ppm (Fondriest Environmental Inc, n.d), the total dissolved solids have to be between 0.028 and 0.25 ppm. This range aligns with the below 0.5 ppm limitation on Total Dissolved Solids (TDS) reported by Ellersdorfer et al (Ellersdorfer et al., 2023). Therefore, an additional step, called water polishing, is necessary to produce high-quality freshwater for all desalination methods to connect them with PEMEL. This step can utilize either an Ion Exchange (IX) or a Continuous Electro Deionisation method (CEDI) (Ellersdorfer et al., 2023).

2.1. Multi-effect distillation

In a MED desalination plant, the term "effect" refers to one of the sequential stages or units through which the feed water passes and is progressively heated and evaporated (Rahimi and Chua, 2017). Similar to the concept of a "plate" or "stage" in a distillation column where the local equilibrium between the liquid and vapour phases is achieved, an "effect" in a MED system is a distinct environment where a portion of the feed water is evaporated into steam, which then condenses to provide heat for the next effect (see also Fig. 4). This cascading effect allows for efficient use of energy and the process is effective at relatively low temperatures by creating vacuum conditions inside the effects.

To optimize efficiency, scale management, and operational responsiveness, various MED configurations have been designed, including backward feed (BF), forward feed (FF), parallel feed (PF), and parallel/cross feed (PCF). BF and FF have counter-current and co-current feedwater flows, respectively, affecting scale formation and response times to disturbances (Elsayed et al., 2018). PF operates at uniform pressure levels for stability, while PCF combines PF and cross-feed features for enhanced thermal efficiency (Elsayed et al., 2018). Integrating Thermal Vapour Compression (TVC) and Mechanical Vapour Compression (MVC) with these configurations further boosts performance (Ettouney et al., 1999). TVC requires high-quality steam for vapour recycling, enhancing thermal efficiency, while MVC utilizes electrical energy for precise control and reduced external energy needs, making it potentially more suitable for scenarios with excess electricity.

Different metrics can be introduced to quantify the efficiency of the MED process. The "Gain Output Ratio" (GOR) is a dimensionless measure of the amount of distillate produced per unit of steam input, expressed as (Al-Shammiri and Safar, 1999):

$$GOR = \frac{\sum_{i=1}^{n} D_i}{m_s} \tag{1}$$

where D_i is the mass flow rate of distillate produced in the " i^{th} " effect, and m_s is the flow rate of steam entering the first effect. The steam consumed in the process is an indirect measurement for the amount of energy being used for desalination. The "Specific Heat Consumption" (SHC), indicating the ratio between energy released by steam condensation at first effect and the total amount of distillate produced, typically calculated as (Darwish et al., 2006):

$$SHC = \frac{2330kJ/kg}{GOR} \tag{2}$$

where the numerator is the latent heat of saturated steam at 65°C. The Specific Heat Transfer Area (S_a) determines the total heat transfer area required per unit of distillate production:

$$S_a = \frac{\sum_{i=1}^{n} A_{e_i} + A_c}{\sum_{i=1}^{n} D_i}$$
 (3)

where A_{e_i} , A_c are the required heat transfer areas for " i^{th} " effect and condenser, respectively.

$$A_{e_i} = \frac{Q_i}{U_{e_i} \times LMTD_i} \tag{4}$$

with Q_i and U_{e_i} determined using equations available in Table 2, and $LMTD_i$ is the logarithmic mean temperature:

$$LMTD_{i} = \frac{(T_{v_{i}} - T_{f}) - (T_{v_{i}} - T_{i})}{\ln(\frac{T_{v_{i}} - T_{f}}{T_{v_{v}} - T_{i}})}$$
(5)

 T_{v_i} and T_f are the vapour and feed water temperature entering the effect, and T_i is the brine temperature leaving the effect. Similar calculation applies for A_c with the temperature of cooling water at the condenser being the seawater temperature (T_{sw}) that it heats up to the cooling water temperature (T_{cw}) .

2.2. Proton exchange membrane electrolysers

A PEM Electrolyser (PEMEL) is an advanced technology for producing hydrogen gas from water using electrical energy. As schematically shown in Fig. 2, a PEM only allows positive hydrogen ions (protons) to pass through while electrons travel around an external circuit, creating an electric current. The primary reactions in PEM electrolysis are (Aouali et al., 2017):

2
$$H_2O(l) + Electricity \rightarrow 2$$
 $H_2(g) + O_2(g) + Heat$ (6)

At the anode, water is oxidised to produce oxygen, protons, and electrons:

2
$$H_2O(l) \rightarrow O_2(g) + 4H^+(aq) + 4e^-$$
 (7)

At the cathode, protons are reduced to hydrogen gas, utilising the electrons from the external circuit:

$$4H^{+}(aq) + 4e^{-} \rightarrow 2 \quad H_{2}(g)$$
 (8)

PEMELs are able to operate at high current densities, making them suitable for large-scale hydrogen production (Shiva Kumar and Himabindu, 2019; Villagra and Millet, 2019). In addition, PEMELs can ramp up and down their hydrogen output, compatible with intermittent power sources like wind and solar, therefore making them attractive for green hydrogen production (Marshall et al., 2007). Note that not all the electrical energy supplied to an electrolyser is used for the water-splitting reaction. In fact, some of this energy is lost as waste heat due to various inefficiencies in the system, such as ohmic resistances and activation overpotentials. The energy required for the water-splitting reaction ($E_{reaction}$) is based on the thermodynamic requirement for splitting water into hydrogen and oxygen, conventionally represented by the hydrogen HHV (High Heating Value), that is approximately 39.4 kWh/kg, and reads as (Bailón et al., 2021):

$$E_{reaction} = m_{H_2} \times HHV_{H_2} \tag{9}$$

where m_{H_2} is the mass of hydrogen produced. Accordingly, assuming an energy input (from e.g., wind turbines) E_{input} , the waste heat (Q_{waste}) generated by the electrolyser is:

$$Q_{waste} = E_{input} - E_{reaction} \tag{10}$$

By substituting the values of E_{input} and E_{useful} from the equations above, we can calculate the waste heat generated by the electrolyser. Commercial PEM electrolysers typically consume around 47–55 kWh per kilogram of hydrogen produced. Under standard operating conditions, this results in approximately 7.6–15.6 kWh/kg H₂ of waste heat,

Energy Reports 14 (2025) 1452–1466

 Table 2

 Main equations of the steady state model (Elsayed et al., 2018; El-Dessouky and Ettouney, 2002).

Thermodynamic Properties Equations (El-Dessou	ıky and Ettouney, 2002)					
Quantity	Equation		Conditions		_	
Latent Heat of Evaporation (kJ/kg)	$h_{fg} = 2501.897 - 2.41 \cdot T + 1.19 \times 10^{-3} \cdot T^2 - 1.59 \times 10^{-5} \cdot T^3$					
Saturated Steam Enthalpy (kJ/kg)	$h_{\rm g} = 2501.69 + 1.81 \times T + 5.88 \times 10^{-4} \times T^2 - 1.22 \times 10^{-5} \times T^3$					
Saturated Water Enthalpy (kJ/kg)	$h_f = -0.0336 + 4.208 \times T - 6.2 \times 10^{-4} \times T^2 + 4.46 \times 10^{-6} \times T^3$					
Saturated Pressure (mbar)	$T_{\text{sat}} = \left(42.6776 - \frac{1}{(\ln(P/10000) - 9.48654)}\right) - 273.15 - \frac{\ln(P_{\text{sat}}/P_c)}{1} = \left(\frac{1}{T + 273.15}\right)$			$T_c = 647.286K$ $P_c = 220890$ mbar		
	$1) \sum\nolimits_{i=1}^8 f_i \cdot (0.01(T+273.15-338.15))^{(i-1)} \begin{array}{ll} f_1 = -7.419242 & f_2 = 0.29721 \\ f_5 = 0.001094098 & f_6 = -0.00439993 \end{array}$	$f_3 = -0.1155286$ $f_4 = 0.008685635$ $f_7 = 0.002520658$ $f_8 = -0.000521868$				
Boiling Point Elevation (°C)	BPE = $A \cdot X + B \cdot X^2 + C \cdot X^3$ $A = 8.325 \cdot 10^{-2} + 1.883 \cdot 10^{-4} \cdot T + 4.02 \cdot 10^{-6} \cdot T^2$ $B = 0.0017 \cdot 10^{-6} \cdot 10^{-6} \cdot 10^{-6}$	$-7.625 \cdot 10^{-4} + 9.02 \cdot 10^{-5} \cdot T - 5.2 \cdot 10^{-7} \cdot T^{2}$ $C =$	0 < X < 16	0ppt 10 < T < 18	0 °C	
	$1.522 \cdot 10^{-4} - 3 \cdot 10^{-6} \cdot T - 3 \cdot 10^{-8} \cdot T^2$					
Specific Heat Capacity of Seawater (kJ/kg.°C)	Specific Heat Capacity of Seawater (kJ/kg. $^{\circ}$ C) $C_p = 10^{-3} \cdot \left(C_0 + C_1 \cdot T + C_2 \cdot T^2 + C_3 \cdot T^3 \right)$ $C_0 = 4206.8 - 6.62 \cdot X + 1.23 \cdot 10^{-2} \cdot X^2$ $C_1 = -1.13 + 5.4 \cdot 10^{-2} \cdot X - 2.27 \cdot 10^{-4} \cdot X^2$ $C_2 = 0.006 \cdot 10^{-3} \cdot $					
	$1.2 \cdot 10^{-2} - 5.36 \cdot 10^{-4} \cdot X + 1.89 \cdot 10^{-6} \cdot X^2 C_3 = 6.88 \cdot 10^{-7} + 1.51 \cdot 10^{-6} \cdot X - 4.43 \cdot 10^{-1} \cdot X - 4.43 \cdot 1$	$^{-9} \cdot X^2$				
			$5989 \times 10^{-5} \times \mathit{T}^2 + 2.5651 \times 10^{-7} \times \mathit{T}^3$			
Overall Heat Transfer Coefficient of Condenser ($U_c = 1.7194 + 3.2063 \times 10^{-3} \times T + 1.5971 \times 10^{-3}$	$^{-5} \times T^2 - 1.99$	$918 \times 10^{-7} \times T^3$		
Steady State Equations for Parallel Feed MED (E						
	First Effect	i th effect	Total	Conservation Eq	uation Used	
Heat Available	$Q_1 = m_s.h_{fg_s}$	$Q_i = D_{i-1}.h_{fg_{(i-1)}}$				
Distillate Produced	$D_i = rac{Q_i}{h_{f\!g_i} + C\!p_f \cdot rac{T_i - T_{f_i}}{1 - \left(rac{X_{f_i}}{X_{b_r}} ight)}}$		$\sum_{i=1}^n D_i$	Mass, Salt, Ener	gy	
Feed Flowrate	$F_i = rac{D_i}{1 - \left(rac{X_{f_i}}{X_{h_i}} ight)}$		$\sum\nolimits_{i=1}^n F_i$	Salt		
Brine Produced	$B_i = F_i - D_i$		$\sum_{i=1}^{n} B_i$	Mass		
Validation of Steady State Model			<i>Z</i> =1 1 1 1 1 1 1 1 1 1 1 1 1 1 1 1 1 1 1			
Validation Source	Input Parameter (kg/s, g/kg, °C)	Variable (kg/s)	Reference	Current Model	Difference (%)	
El-Dessouky (El-Dessouky and Ettouney, 2002)	$T_{sw} = 25$, $X_f = 42$, $X_b = 94$, $n = 4$, $T_f = 35$, $T_{cw} = 31.5$, $T_{bn} = 40$, $m_s = 0.4032$, $T_s = 70$	Distillate Produced	1.39	1.44	+ 3.32 %	
		Feed Flowrate	2.52	2.60	+ 3.23 %	
		Brine Flowrate	1.12	1.16	+ 3.13 %	
Elsayed et al (Elsayed et al., 2018).	$T_{sw} = 25, X_f = 35, X_b = 53, n = 4, T_f = 41.5, T_{cw} = 31.5, T_{bn} = 45.4, m_s = 14.4, T_s = 65$	Distillate Produced	53.63	53.19	-0.82 %	
		Feed Flowrate Brine Flowrate	157.91 104.19	156.61 103.43	$-0.83 \% \\ -0.73 \%$	
		DITHE LIOMISTE	104.19	103.43	-0.73 %	

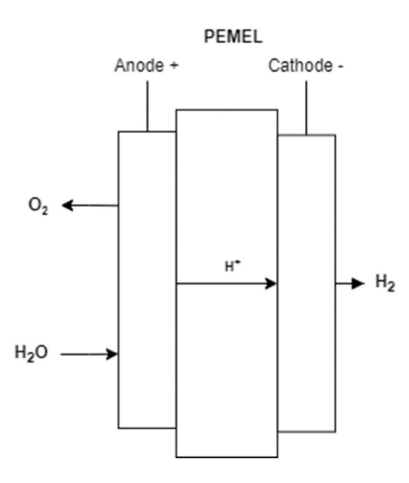


Fig. 2. PEMEL process diagram.

accounting for about 16-28 % of the total energy consumption.

3. Methods

The Python model for process analysis conducted in this study consists of three main steps schematically shown in Fig. 3. a, b, c. In the first step, a steady-state simulation is performed for MED in parallel feed configuration for validation of our model with the studies by Elsayed et al. (Elsayed et al., 2018), and El-Dessouky & Ettouney (El-Dessouky and Ettouney, 2002). In the second step, the validated model is used to define the design characteristics of the MED to cover the maximum demand of 1 GW PEMEL. In the third and last step, an analysis of the operations of the designed MED is performed, in which the water production of MED is calculated based on the waste heat available in the electrolyser for each hour of a representative year of a 1 GW offshore wind farm. For each hourly timestep, the waste heat becomes available based on the PEMEL operations depending on the generated wind power. The effects of variability on pure water generation are therefore assessed and potential water production mismatches are identified. Several sensitivity analyses are also performed.

Additionally, the spatial allocation for technologies in offshore environments is a critical consideration. However, reported values for desalination plants vary significantly across different references. Therefore, in this study, the footprint area required for the MED is estimated by assuming each effect is a shell-and-tube heat exchanger. According to the Tubular Exchanger Manufacturers Association (TEMA) standards, the estimations assume a six-meter shell and square pitch single pass heat exchanger. The outside diameter is calculated based on the total heat transfer area required and used to determine the footprint area in a vertical and horizontal arrangement. The estimated value is then multiplied by two to account for the spatial occupancy of other equipment and maintenance areas.

3.1. Steady state model validation

The steady state model is developed based on literature with Fig. 3a schematically showing the flow of calculations, where equations are solved iteratively to achieve the same heat transfer area for all effects and energy balance at preheaters. The thermodynamic properties of streams are based on the equations of Table 2. These include boiling point elevation, specific heat capacity of seawater, water and vapour enthalpies, and latent heat of evaporation. The overall heat transfer coefficient is calculated at each iteration to derive the required heat transfer area at each effect. After model convergence for the effects, the condenser heat transfer area, MED metrics such as GOR, SHC, S_a , and total distillate production are calculated. Note that the following assumptions are made:

1. The thermodynamic properties of seawater, such as boiling point elevation (BPE) and specific heat capacity (C_p), depend only on temperature and salinity.

- The salinity of the brine is assumed to be constant across all effects, matching the salinity of the final brine.
- 3. The distillate salinity is assumed to be zero, indicating it is salt-free. Despite this is not the case in the real process, due to the low salinity (5 ppm) we do not expect a significant loss of accuracy because of this assumption.
- 4. The impact of non-condensable gases in the vapour on the process is negligible.
- 5. Temperature difference between brine and vapour is equal to BPE.

The model input parameters (to initialise the steady state calculation) are steam temperature (T_s) , Steam Flowrate (m_s) , Seawater Temperature (T_{sw}) , Cooling Water Temperature (T_{cw}) , Feedwater Temperature (T_f) , feedwater salinity (X_f) , brine salinity (X_{b_n}) , number of effects (n), last brine temperature (T_{b_n}) . Among these, T_{sw} and X_f are environmental conditions. Therefore, after validation, these values are replaced with 34 g/kg and 12°C, respectively, to reflect North Sea average characteristics (Swertz et al., 1999; Prandle et al., 1997). Moreover, the number of effects is a design parameter, and the feed temperature is an initial guess. All the other parameters are operation conditions of the MED plant and are maintained constant across all the models. These operating parameters reflect the actual operating plant in Tripoli, which has a capacity of producing 58 kg/s of water (Elsayed et al., 2018; Ashour, 2003).

As shown in Table 2, the MED steady state model is validated against two different studies, obtaining less than 5 % difference in results with sources, confirming the robustness and reliability of our model.

3.2. Modelling

In the design step, the aim is to determine the heat transfer area and other characteristics of the MED system that can support PEM hydrogen generation at maximum load. The electrolyser data is based on state-of-the-art PEM published by the US Department of Energy ("Annual Merit Review Presentation Database," 2024) and scaled for a 1 GW PEM working at 100 % of the nominal load. The waste heat input of the steady state model is then iteratively increased to achieve the same total water production as the maximum water demand of the electrolyser (see flowchart in Fig. 3b). After convergence, the obtained design parameters are to be used in the operation analysis. Furthermore, this model is used to identify the optimal number of effects. An additional sensitivity related to the possibility of "over/under-design" the system is performed, to assess how this impacts the number of hours for which electrolyser water supply is insufficient.

Because the waste heat in PEMEL cooling water is not vapourised, converting the waste heat energy available to the corresponding steam flow rate and temperatures is a necessary step before starting the MED calculations. Therefore, a simple model for a connector evaporator named "effect number zero" is developed to couple the PEM data and the MED steady state model. Here, the PEM is assumed to operate at 80°C with a 5°C ($\Delta T_{PEM}=80-75$) temperature difference between inlet and outlet of PEM cooling water (see also Fig. 4). Then, the amount of steam generated at 10°C ($\Delta T_S=75-65$) lower than the PEM cooling water temperature is calculated as shown in Fig. 3d. Consequently, the steam temperature entering the first effect is 65°C ($T_S=80-\Delta T_{PEM}-\Delta T_S=65$ °C). Later, a sensitivity analysis will be performed to assess how temperature differences impact the zero-effect size and the required vacuum pressure.

Next, an analysis of the operations of the designed MED is conducted, based on the flowchart of Fig. 3c. Hourly wind power generation is calculated based on the Netherlands offshore wind data from 2017 (Koninklijk Nederlands Meteorologisch Instituut (KNMI), 2023), scaled

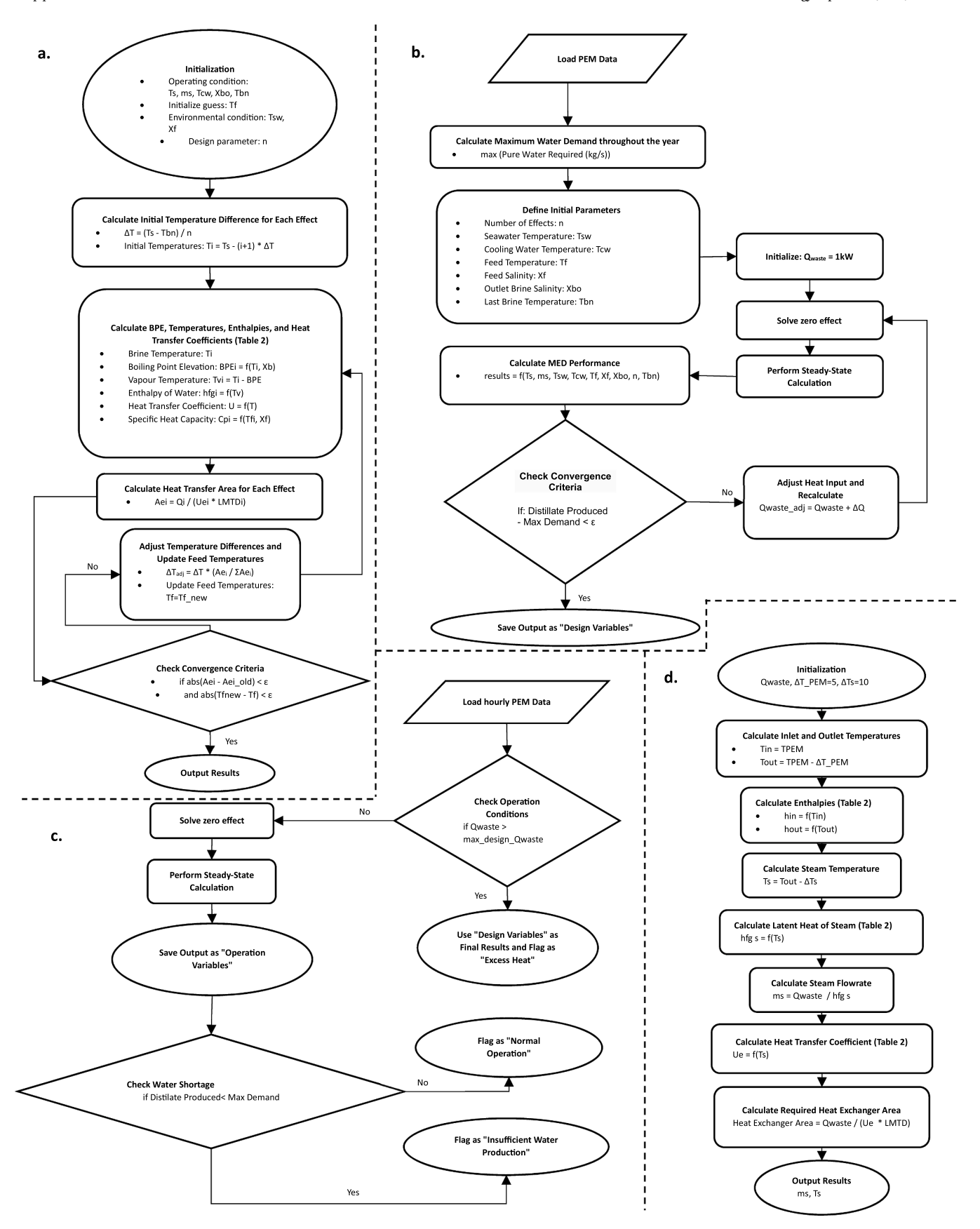


Fig. 3. The flowcharts of the process simulation for a. steady state b. design c. operation models d. zero effect.

to 1 GW offshore wind farm. A 1-to-1 wind power installed capacity to PEM electrolysis installed capacity (e.g., 1 GW wind power to 1 GW electrolysis) is assumed. The available waste heat in the electrolyser is calculated as described above and a quasi-steady-state model is used to calculate the hourly water production of the designed MED. Three main operating conditions are recorded at each hourly time step for the integrated system when wind generation is not zero:

- Excess Heat: If the available PEMEL waste heat is higher than the maximum amount allowed for the designed MED. The excess heat is calculated and stored in the results.
- 2. **Normal Operation:** The steady state model is solved with the actual value of the waste heat (that is smaller than the maximum allowed). In this case, the calculated distillate production is higher than the PEM water requirement.
- Insufficient Water Production: In this case, the distillate production based on the steady state model is less than the electrolyser water demand.

When the wind generation is zero, the system is flagged as nonoperational.

4. Results and discussion

The steady state process diagram of the four-effect MED system plus effect number zero with corresponding flowrates and temperatures of the streams is shown in Fig. 4. The system achieves a total water production rate of 50.64 kg/s with a total feed water usage of 141.25 kg/s. It also produces 90.62 kg/s of brine at 41.5°C, which still is an environmental challenge for the disposal at the sea (Ahmad and Baddour, 2014). The *GOR*, *SHC*, S_a are about 3.69, 631.54 kJ/kg, and 155.12 m²/kg/s, respectively (see Table 3).

To highlight the potential water production of MED, the steady state model was solved for various waste heat energy and temperature to obtain the design plane of Fig. 5.a. Based on the data available in Steinbach (Steinbach, 2023) a gigawatt-scale electrolyser at 80°C and nominal load would generate 134.37 MW (red plane) of waste heat and consume 50.64 kg/s (blue plane) of water to produce hydrogen. Although the waste heat is lower than the value reported elsewhere (171.1 MW) (Joris, 2019), the energy consumption/waste heat value was chosen to reflect the current state of the art of PEMEL (which corresponds to 46.9 kWh/kg at 100 % baseload cf (Steinbach, 2023), and the analysis reveals that the waste heat produced is already significantly higher than the thermal energy required to meet the water demand of the PEM electrolyser.

Fig. 5b. examines the influence of the number of effects on different

Table 3Main metrics of the designed MED.

Parameter	Symbol	Value	Unit
Total water production rate	$\sum_{i=1}^4 D_i$	50.64	kg/s
Total feed water usage	$\sum_{i=1}^{l-1} F_i$	141.25	kg/s
Total brine production	$\sum_{i=1}^{l-1} B_i$	90.62	kg/s
Seawater Intake	m_{sw}	375.52	kg/s
Gain Output Ratio	GOR	3.69	-
Specific Heat Consumption	SHC	631.54	kJ/kg
Specific Area	S_a	155.12	m ² /kg/s
Heat Transfer Area Effect 0	A_{e_0}	1061.30	m ²
Heat Transfer Area of Effect 1-4	A_{ei} $(i = 1to4)$	1372.53	m^2
Heat Transfer Area of Condenser	A_c	1303.86	m^2
Total Heat Transfer Area	A_{total}	7855.28	m ²
Vertical footprint area	-	22.78	m^2
Horizontal footprint area	-	129.94	m ²

parameters related to the designed MED. While increasing the number of effects generally enhances the efficiency of water recovery (GOR) and reduces the energy per unit of distillate (SHC), it also necessitates a larger heat transfer area. Therefore, the optimal number of effects could be around n values of 2 and 4. Additionally, the analysis considers the average saturated/vacuum pressure (Pv_{Ave}), calculated from the temperatures across all effects. The data shows a logarithmic increase in the required vacuum level, which implies higher operational energy requirements for vacuum pumps in systems with more effects. This leads to higher energy consumption in vacuum pumps, making the configurations with more effects less attractive. For the rest of this work, we decided to further study the MED system with four effects. This choice represents a balance between maximizing thermal and water recovery efficiencies and minimizing the costs and complexities of larger systems.

Fig. 6.a. shows the hourly water production and consumption throughout the sample year. The data has been resampled for 7-hour intervals to smooth the curves for a clearer presentation. Analysis indicates that there are a few hours with water production shortages, while many hours show water production exceeding the demand from PEMEL. Where the hours with a shortage of supply are highlighted in Fig. 6b., the maximum continuous period of water shortage happens on the 8th of Nov between 04:00 and 23:00. During this period, the required water storage volume to meet the demand is calculated to be 2.23 m³. This small storage capacity indicates minimal operational limitations under this design scenario. To understand the context better, the electrolyser volume is around 50 m³/MW (Inc, 2021). Thus, this storage capacity is around 0.004 % of the space a 1 GW electrolyser occupies. However, this storage capacity could still be significant in an offshore environment as it poses a risk of sloshing and other installation

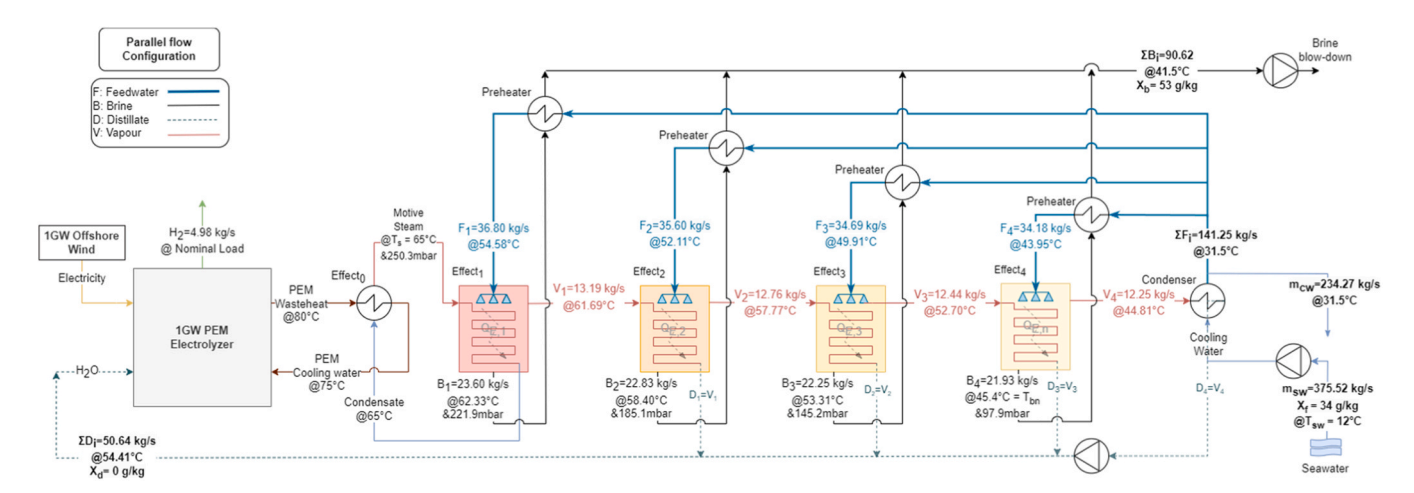


Fig. 4. The process flow diagram of MED with mass flow rates and temperatures designed to cover PEMEL working at 80°C and 100 % of nominal load.

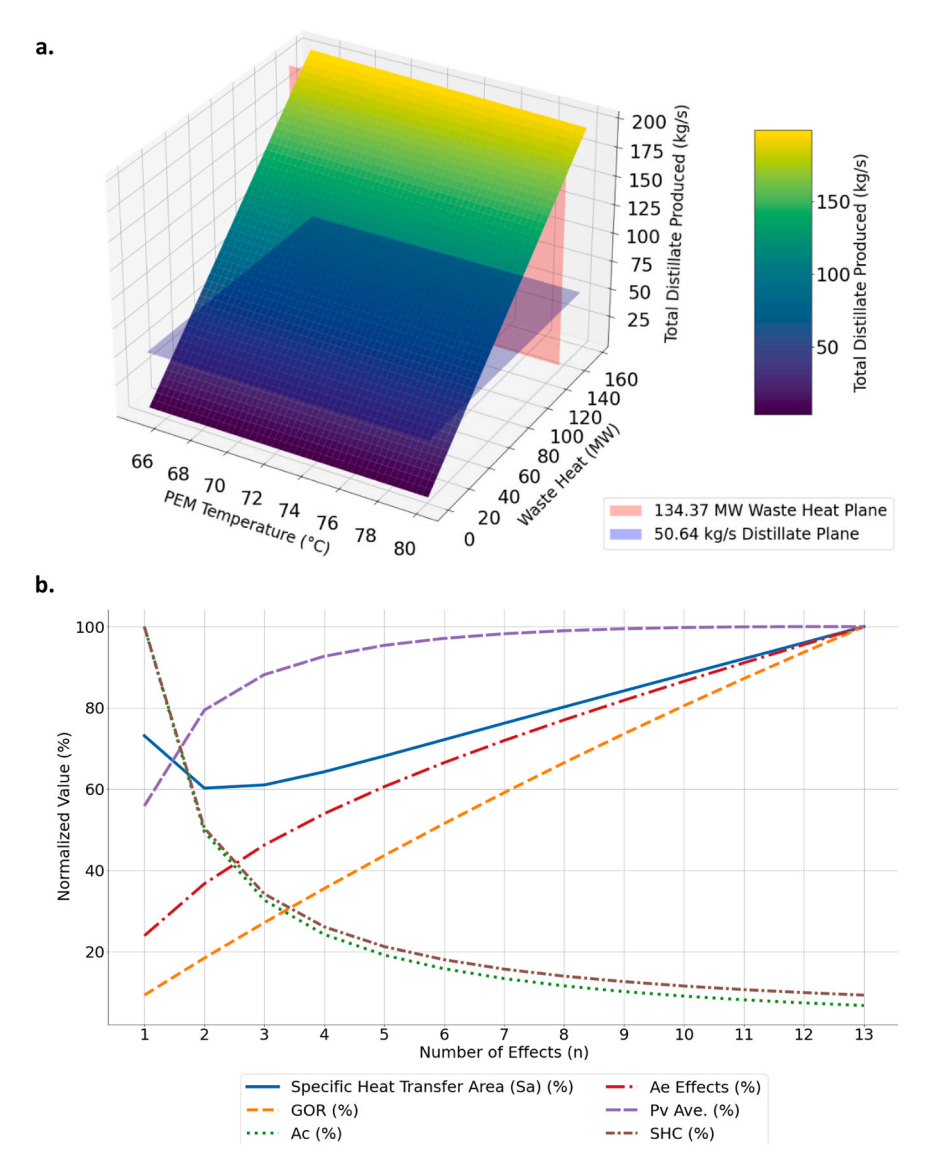


Fig. 5. Design properties of the MED system a. design plane for possible integration b. different number of effects.

considerations.

The integrated system operation demonstrates minimal sensitivity to variations in stack temperature, as shown in Fig. 6c. It is important to note that the water requirement in the PEM is assumed constant while only stack temperatures are adjusted to assess their impact on periods when the water supply falls short. In real-world conditions, stack performance fluctuates with temperature changes, suggesting that water consumption should be recalculated accordingly.

Additionally, Fig. 6d. examines the consequences of over- and under-designing the MED relative to the maximum demand for PEMEL. Notably, under-designing significantly impacts the number of hours when water production fails to meet demand. However, overdesign offers no benefits, as the data remains unchanged even when the over-design percentage is increased to 3 %. This lack of change is mainly because the periods of shortage often occur when waste heat availability is low, which typically coincides with reduced wind activity and, consequently, lower power input to the electrolyser.

Fig. 7 presents operational data for the electrolyser, sorted by the power input. The PEMEL produces 4.98 kg/s of green hydrogen at maximum load and requires 50.64 kg/s of pure water. It is observed that above 600 MW, or 60 % of the nominal load, the waste heat available from the stack exceeds the amount required by the MED. In situations of

excess heat generation, additional cooling systems must be in place to maintain safe operating temperatures for the electrolyser. On the other hand, water shortages occur when the electrolyser operates below 50.6 MW, approximately 5 % of the nominal load. Notably, the electrolyser is typically shut down when operating below 10 % of its capacity due to increased hydrogen crossover in these operating conditions, which will consequently increase the risk of forming an explosive mixture. Therefore, it can be inferred that both the water supply limitations and the shortage periods depicted in Fig. 6d. occur when the electrolyser system is not operational.

As mentioned, to integrate MED with PEMEL, effect number zero is developed with assumptions for temperature differences in PEM cooling water and steam generated. Fig. 8 examines the sensitivity of these parameters to the system design attributes, namely the heat transfer area and vacuum pressure required for the process. As expected, Fig. 8a. suggests that increasing temperature differences decrease the heat transfer area of the effect and consequently offer lower cost and spatial requirements for equipment. On the other hand, Fig. 8b. shows that assuming higher temperature differences increases the vacuum pressures required, potentially raising the operation cost to maintain vacuum conditions and better sealing in the equipment. Therefore, a promising avenue exists to analyse the optimum temperature differences

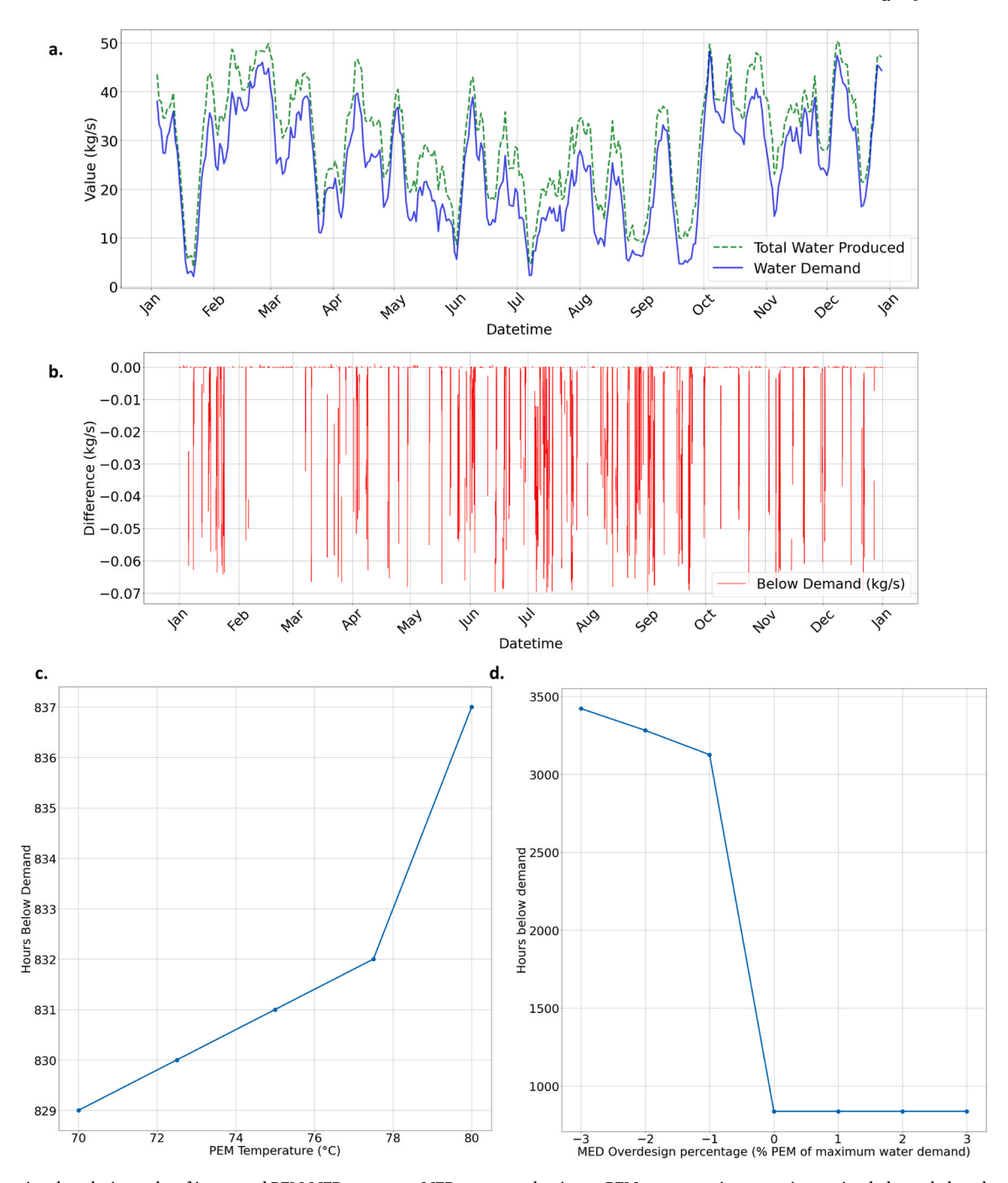


Fig. 6. Operational analysis results of integrated PEM-MED system. a. MED water production vs PEM water requirements time series. b, hours below demand for the sample year. c. PEM temperature variation on hours below demand. d. effect of MED overdesign percentage on the hours below demand.

based on investment and operation costs in future studies.

4.1. Spatial and environmental requirements

The footprint area calculated with this model is $129.94 \, \mathrm{m}^2$ in a horizontal arrangement and $22.78 \, \mathrm{m}^2$ in a vertical arrangement. To clarify the context, according to the HyBalance report, a 25 MW PEMEL has a footprint of approximately 297.68 m^2 (equivalent to ten 40 ft containers) (Thomas, 2019). Therefore, a 1 GW PEMEL would require $11907 \, \mathrm{m}^2$ of land for installation. Although this estimate does not include the optional utilities mentioned in the report, the footprint required by PEMEL is significantly higher than that of MED. Comparing this with manufacturer data, the NEL MC500 model has a specific

footprint of 22.70 m²/MW if the units are placed next to each other and 11.35 m²/MW if stacked (nel, 2020), while the Cummins HyLyzer 500 has similar values (Inc, 2021). The Plug EX-425D model, on the other hand, shows a specific footprint of 36.57 m²/MW (Plug, 2024). These comparisons suggest that the estimate of 12000 m²/GW is reasonable but slightly on the lower end.

To standardise and compare data, the reported footprint area of each plant is divided by its distillate production, yielding a specific footprint area. The first bar in Fig. 9 shows the average specific footprint for desalination plants, as noted by Voutchkov (Voutchkov, 2012). According to Voutchkov this value decreases with increasing production scale (Voutchkov, 2012). This trend, which aligns with expectations for most technologies, suggests that larger plants are more space efficient.

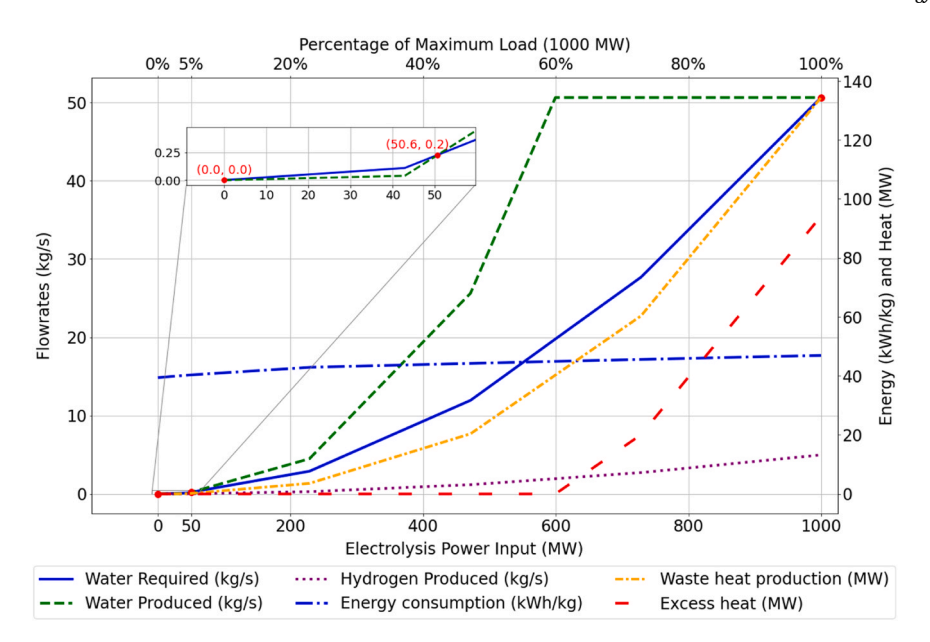


Fig. 7. PEMEL operational parameters and water production vs electrolyser load.

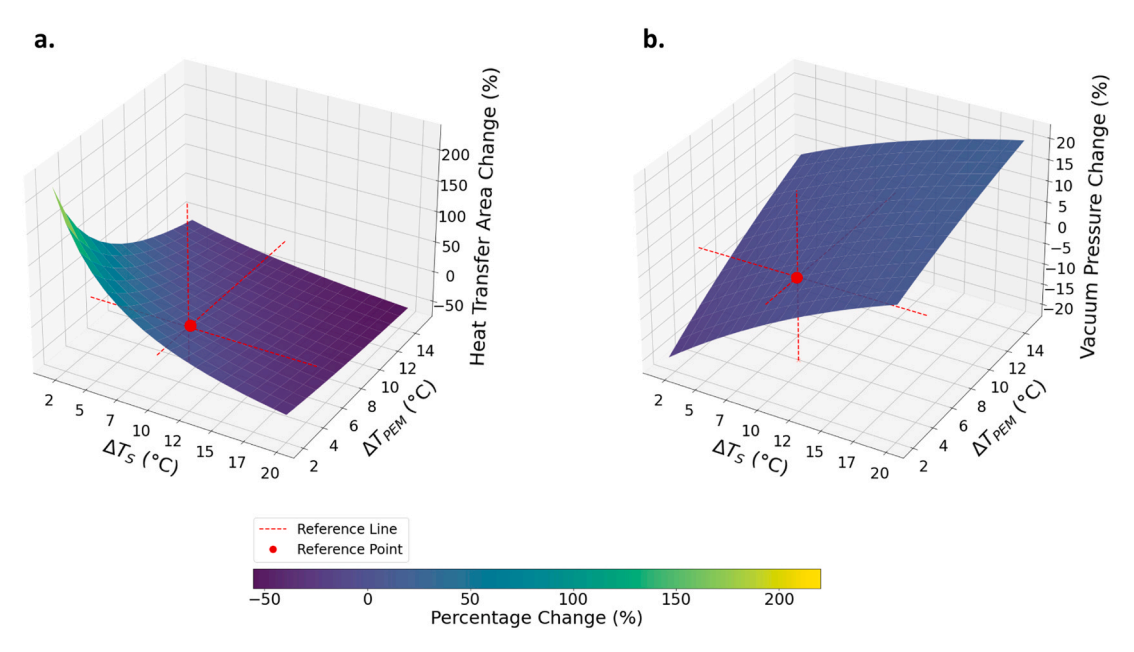


Fig. 8. Specific footprint area of MED from different sources and comparison between the current model's results (Adak and Tewari, 2014; Voutchkov, 2012; Herber, 2024).

While this book mentions a range of up to 3500 kg/s for desalination plants, the type of plant is not specified, adding a layer of uncertainty to this comparison.

The second and third bars data are derived from an article comparing reverse osmosis with MED, indicating that MED requires twice the land area of RO for 4380 kg/s of water production (Herber, 2024). Finally, the fourth and fifth bars represent the specific footprint from the proposed model, aligning closely with the data from the sixth bar, which represents a more compact MED with TVC (Adak and Tewari, 2014). Because the GOR of MED-TVC plants is typically higher than that of standalone MED, they have a lower specific footprint area. It is crucial to note that the estimated footprint in the current study does not account for the zero effect. Additionally, even in a system without desalination, a larger heat exchanger is necessary to cool down the electrolyser waste heat before disposal.

While there is still uncertainty around the footprint area of the designed MED, other findings suggest that such integration is technically operable. Additionally, integrating MED into the system is beneficial regarding environmental impact. Meanwhile, the literature suggests that higher release points for brine disposal can help reduce its environmental impact on the marine ecosystem (Blackford et al., 2021). According to another source, marine benthic algae in the North Sea, such as those near Helgoland, tolerate temperatures ranging between 0°C and 28°C, with no species surviving above 33°C (Lüning, 1984). Integrating MED reduced the temperature of the disposal stream from 80°C to 41.5°C but increased salinity from 34 to 53 g/kg. However, this increased salinity seems more manageable (Sola et al., 2020).

Additionally, 234.27 kg/s of seawater at 31.5°C is generated to cool down the condenser. This heated byproduct must also be cooled before disposal. Although this falls outside the scope of this study, it presents an

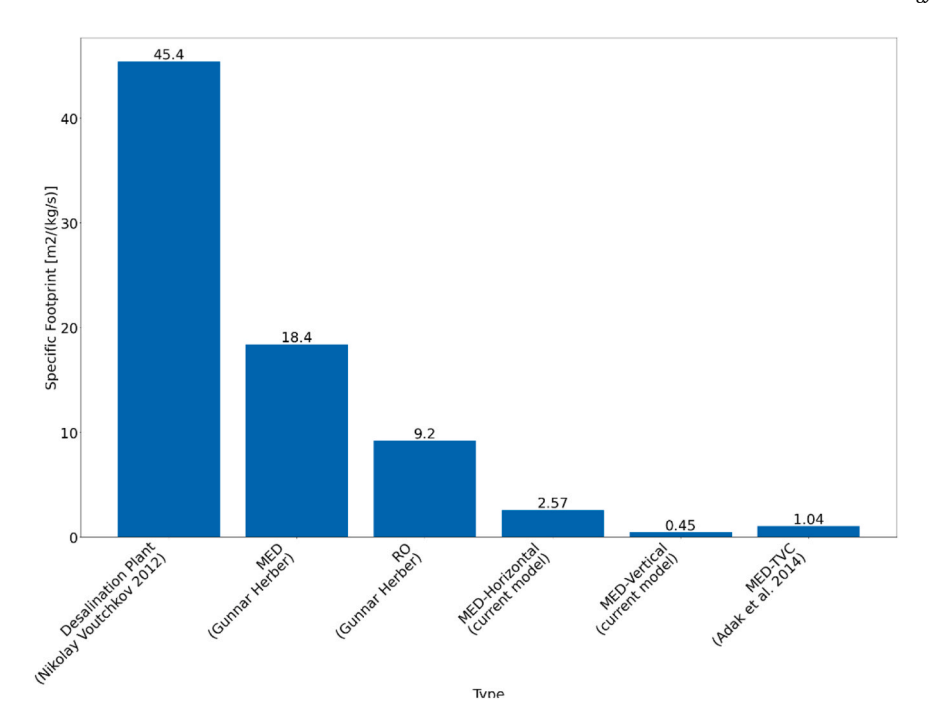


Fig. 9. Sensitivity analysis of effect number zero on the impact of temperature differences in PEM cooling water and steam entering the first effect on a. heat transfer area and b. vacuum pressure. (At the reference point: $\Delta T_{PEM} = 5^{\circ}C$, $\Delta T_{S} = 10^{\circ}C$, $A_{0} = 1061.30$ m^{2} , $P_{v} = 250.3$ mbar).

opportunity to further reduce environmental impact. This stream can be used to cool and dilute the brine. However, even then, the system still requires an additional heat exchanger to lower the temperature to environmentally safe levels before disposal because the mixed stream (condenser cooling water and brine) ends up with a combined flow of 324.89 kg/s (respectively 234.27 kg/s + 90.62 kg/s) with a salinity of 39.3 g/kg at 34.3°C (North sea condition: X_f =34 g/kg, T_{sw} =12°C).

4.1.1. Limitations

Although the assumptions made in this study simplify the modelling process, they introduce certain limitations that may impact the accuracy and applicability of the results. Simplifying the thermodynamic properties and process conditions may not capture the full complexity of real-world scenarios, potentially leading to discrepancies between the model predictions and actual performance. Treating salinity uniformly might add small, cumulative effects that can influence system performance. Additionally, assuming ideal water purity may not fully represent practical conditions where traces of impurities are present. Addressing these limitations in future work could enhance the model robustness and provide a more realistic representation of the multi-effect distillation process. Furthermore, although this study does not consider the preheater heat transfer area, its significance might be high due to the low-temperature difference between the hot and cold streams, especially in the final effects.

The designed system aims to cover the maximum water demand for PEMEL's operation. However, this approach results in many hours throughout the year when water production exceeds demand. This suggests an opportunity to design a water storage tank to support hydrogen production alongside MED. Implementing such a tank would allow for a smaller desalination plant, which is advantageous for offshore platforms where spatial allocation is crucial. On the other hand, lower usage of waste heat can increase the working load on the auxiliary cooling heat exchanger and lead to more hot water being disposed of into the sea. While this reduces the amount of brine disposal, which is beneficial for the environment, the increased hot water disposal has negative environmental impacts. Therefore, it is essential to balance water production, storage capacity, and environmental considerations to ensure sustainable and efficient operation.

According to the operation results, there are no significant limitations on the operation of the integrated system. However, there are still some questions related to the actual dynamic behaviour of the system in the real-life scenario, like the ramping up and down of PEM on the MED. A quasi-steady-state model cannot replicate such system behaviours, and a transient model must be developed to analyse these situations better. Moreover, this study does not consider the maintenance downtime and the degradation of the performance of the systems, which can lead to an overestimation of the system performance.

To enhance the accuracy of the results, future work should consider revisiting the assumptions made for the steady-state model and developing a transient model for both MED and PEMEL systems. This approach would allow for a more accurate prediction of system behaviour, particularly during ramping up and down scenarios. Additionally, modelling alternative desalination technologies such as RO or MSF could provide valuable comparisons and help identify the best technology for different operational situations. Further design optimisation, based on previous suggestions, is recommended to ensure the most efficient integration of PEM electrolysers with MED systems.

For managers of offshore renewable energy projects, this integration offers a viable strategy to improve hydrogen production efficiency. This approach can facilitate simultaneous water and hydrogen production on offshore platforms. Furthermore, water scarcity may become more pressing in the region. In that case, policymakers should consider incentivising the development of combined renewable energy and desalination technologies and adapting regulatory frameworks to support the deployment of these integrated systems. In such a situation, the results of this study can guide them through this process. Promoting these innovative solutions aligns with national and international climate goals, addresses water security challenges, and supports the transition to a sustainable energy future.

5. Conclusion

This work is the first to assess, in detail, the technical feasibility of coupling a 1 GW offshore PEM electrolyser with a multi-effect distillation (MED) unit that re-uses the stack's low-grade (≈ 80 °C) waste heat to produce its own process water. By uniting waste-heat recovery, dynamic

wind-driven operation and footprint analysis in a single model, the study extends earlier onshore or steady-state investigations.

A quasi-steady-state MED model was built, validated against published plant data, and driven by hourly Dutch offshore-wind power profiles. Design variables included a number of effects (n), condenser pressure, and heat-exchange area. Performance was tracked via gain-output ratio (GOR), specific heat consumption (SHC), specific area (S_a) , distillate/brine flowrates, unused heat, and platform footprint.

- A four-effect MED meets the full water demand (50.6 kg/s) of a 1 GW PEM electrolyser operating at 80 °C.
- Achieved GOR = 3.69, SHC = 632 kJ/kg, and $S_a = 155$ m²/kg/s, confirming competitive thermodynamic performance.
- The MED lowers the cooling-water outlet to 41.5 °C but this 90.6 kg/s produced brine, raises local salinity and requiring discharge management.
- MED reuses 40 MW of the electrolyser waste heat; 94 MW remain when the stack load exceeds 60 %, indicating scope for auxiliary heat-recovery or cooling solutions.
- Over-design of the MED has little benefits, whereas under-design leads to frequent water shortages.
- Estimated platform footprint is around 130 m² (horizontal layout) or 23 m² (compact vertical layout), feasible for North-Sea installations.

The analysis assumes vacuum maintenance and neglects detailed brine-dispersion modelling; economic metrics were not included. Future studies should (i) optimise MED sizing jointly with short-term water storage, (ii) evaluate hybrid heat-recovery options for the 94 MW surplus, (iii) couple the model to cost and life-cycle assessments, and (iv) perform site-specific ecological studies on elevated-salinity discharge in sensitive offshore ecosystems.

The findings suggest that such integration is technically operable and thus can optimise resource utilisation and mitigate the environmental impacts of waste heat disposal. The knowledge gathered from this research can direct future efforts to create green hydrogen production platforms that are more efficient and sustainable.

Author statement

We the undersigned declare that this manuscript is original, has not been published before and is not currently being considered for publication elsewhere. We confirm that the manuscript has been read and approved by all named authors and that there are no other persons who satisfied the criteria for authorship but are not listed. We further confirm that the order of authors listed in the manuscript has been approved by all of us. We understand that the Corresponding Author is the sole contact for the Editorial process. He/she is responsible for communicating with the other authors about progress, submissions of revisions and final approval of proofs.

Declaration of Competing Interest

The authors declare that they have no known competing financial interests or personal relationships that could have appeared to influence the work reported in this paper.

Acknowledgements

We acknowledge Prof. Matteo Gazzani (Utrecht University) for useful discussions and support in the graduation project of M.H.

Data availability

No data was used for the research described in the article.

References

- "Annual Merit Review Presentation Database," *US Department of Energy*, 2024. (https://www.hydrogen.energy.gov/amr-presentation-database.html).
- Adak, A.K., Tewari, P.K., 2014. Technical feasibility study for coupling a desalination plant to an Advanced Heavy Water Reactor. Desalination 337 (1), 76–82. https:// doi.org/10.1016/j.desal.2013.11.004.
- Ahmad, N., Baddour, R.E., 2014. A review of sources, effects, disposal methods, and regulations of brine into marine environments. Ocean Coast. Manag 87, 1–7. https://doi.org/10.1016/j.ocecoaman.2013.10.020.
- Ahmed, M., Shayya, W.H., Hoey, D., Al-Handaly, J., 2001. Brine disposal from reverse osmosis desalination plants in Oman and the United Arab Emirates. Desalination 133 (2), 135–147. https://doi.org/10.1016/S0011-9164(01)80004-7.
- Al-Mutaz, I.S., 1996. A comparative study of RO and MSF desalination plants.

 Desalination 106 (1–3), 99–106. https://doi.org/10.1016/S0011-9164(96)00097-5.
- Al-Sahali, M., Ettouney, H., 2007. Developments in thermal desalination processes: Design, energy, and costing aspects. Desalination 214 (1–3), 227–240. https://doi. org/10.1016/j.desal.2006.08.020.
- Al-Shammiri, M., Safar, M., 1999. Multi-effect distillation plants: State of the art.

 Desalination 126 (1–3), 45–59. https://doi.org/10.1016/S0011-9164(99)00154-X.
- W.A. Amos, "Costs of Storing and Transporting Hydrogen," 1999. [Online]. Available: http://www.ostj.gov/bridge/servlets/purl/6574-OBMIFS/webyjewable/)
- Aouali, F.Z., Becherif, M., Ramadan, H.S., Emziane, M., Khellaf, A., Mohammedi, K., 2017. Analytical modelling and experimental validation of proton exchange membrane electrolyser for hydrogen production. Int. J. Hydrog. Energy 42 (2), 1366–1374. https://doi.org/10.1016/j.ijhydene.2016.03.101.
- Ashour, M.M., 2003. Steady state analysis of the Tripoli West LT-HT-MED plant. Desalination 152 (1–3), 191–194. https://doi.org/10.1016/S0011-9164(02)01062-7
- Atlas High Purity Solutions team, 2019. ASTM and ISO Water Quality Standards for Laboratory-Grade Water. Atlas High. Purity Solut. (https://forum.atlashighpurity.com/blog/astm-and-iso-water-quality-standards-for-laboratory-grade-water).
- com/blog/astm-and-iso-water-quality-standards-for-laboratory-grade-water).

 R. Bailón, J. Rodríguez, and A. Woocay, "Energy Efficiency Analysis of a PEM Electrolyzer and a PEM Hydrogen Fuel Cell," 2021.
- Bamufleh, H., Abdelhady, F., Baaqeel, H.M., El-Halwagi, M.M., 2017. Optimization of multi-effect distillation with brine treatment via membrane distillation and process heat integration. Desalination 408, 110–118. https://doi.org/10.1016/j. desal.2017.01.016
- Barbir, F., 2005. PEM electrolysis for production of hydrogen from renewable energy sources. Sol. Energy 78 (5), 661–669. https://doi.org/10.1016/j. solener.2004.09.003.
- Blackford, J., Dewar, M., Espie, T., Wilford, S., Bouffin, N., 2021. Impact potential of hypersaline brines released into the marine environment as part of reservoir pressure management. 15th Greenh. Gas. Control Technol. Conf. 2021 GHGT 2021 (March). https://doi.org/10.2139/ssrn.3821554.
- Brogioli, D., La Mantia, F., Yip, N.Y., 2018. Thermodynamic analysis and energy efficiency of thermal desalination processes. Desalination 428 (July 2017), 29–39. https://doi.org/10.1016/j.desal.2017.11.010.
- Brosschot, S., 2022. Comp. Hydrog. Netw. Electr. grids Transp. Offshore Wind Energy shore North Sea Reg. A Spat. Netw. Optim. Approach.
- A. Buljan, "The Netherlands Chooses Site for World's Largest Offshore Wind-to-Hydrogen Project."(n.d) (https://www.offshorewind.biz/2023/03/20/the-netherlands-chooses-site-for-worlds-largest-offshore-wind-to-hydrogen-project/).
- Buttler, A., Spliethoff, H., 2018. Current status of water electrolysis for energy storage, grid balancing and sector coupling via power-to-gas and power-to-liquids: A review. Renew. Sustain. Energy Rev. 82 (September 2017), 2440–2454. https://doi.org/10.1016/j.rser.2017.09.003.
- Curto, D., Franzitta, V., Guercio, A., 2021. A review of the water desalination technologies. Appl. Sci. 11 (2), 1–36. https://doi.org/10.3390/appl11020670.
- Darwish, M.A., Al-Juwayhel, F., Abdulraheim, H.K., 2006. Multi-effect boiling systems from an energy viewpoint. Desalination 194 (1–3), 22–39. https://doi.org/10.1016/ j.desal.2005.08.029.
- van der Roest, E., Bol, R., Fens, T., van Wijk, A., 2023. Utilisation of waste heat from PEM electrolysers Unlocking local optimisation. Int. J. Hydrog. Energy 48 (72), 27872–27891. https://doi.org/10.1016/j.ijhydene.2023.03.374.
- Do Thi, H.T., Pasztor, T., Fozer, D., Manenti, F., Toth, A.J., 2021. Comparison of Desalination Technologies Using Renewable Energy Sources with Life Cycle, PESTLE, and Multi-Criteria Decision Analyses. Water 13 (21). https://doi.org/ 10.3390/w13213023.
- El-Dessouky, H.T., Ettouney, H.M., 2002. Fundam. Salt Water Desalin.
- Ellersdorfer, P., Omar, A., Taylor, R.A., Daiyan, R., Leslie, G., 2023. Multi-effect distillation: a sustainable option to large-scale green hydrogen production using solar energy. Int. J. Hydrog. Energy 48 (81), 31491–31505. https://doi.org/10.1016/j.ijhydene.2023.04.261.
- Elsaid, K., Taha Sayed, E., Yousef, B.A.A., Kamal Hussien Rabaia, M., Ali Abdelkareem, M., Olabi, A.G., 2020. Recent progress on the utilization of waste heat for desalination: A review. Energy Convers. Manag 221 (April), 113105. https://doi. org/10.1016/j.enconman.2020.113105.
- Elsayed, M.L., Mesalhy, O., Mohammed, R.H., Chow, L.C., 2018. Transient performance of MED processes with different feed configurations. Desalination 438 (December 2017), 37–53. https://doi.org/10.1016/j.desal.2018.03.016.
- Erickson, L.E., Brase, G., 2019. Paris Agreement on Climate Change. in Reducing Greenhouse Gas Emissions and Improving Air Quality. CRC Press, Boca Raton, pp. 11–22. https://doi.org/10.1201/9781351116589-2.

Ettouney, H., El-Dessouky, H., Al-Roumi, Y., Apr. 1999. "Analysis of mechanical vapour compression desalination process," (doi). Int. J. Energy Res 23 (5), 431–451. https://doi.org/10.1002/(SICI)1099-114X(199904)23:5<431::AID-ER491>3.0.CO;2-S.

- European Commission, "The European Green Deal," 2019. [Online]. Available: (https://commission.europa.eu/strategy-and-policy/priorities-2019-2024/european-green-deal en).
- Fondriest Environmental Inc., "Conductivity, Salinity & Total Dissolved Solids,"(n.d) fundamentals of Environmental Measurements. (https://www.fondriest.com/environmental-measurements/parameters/water-quality/conductivity-salinity-tds/).
- Fritzmann, C., Löwenberg, J., Wintgens, T., Melin, T., 2007. State-of-the-art of reverse osmosis desalination. Desalination 216 (1–3), 1–76. https://doi.org/10.1016/j.desal.2006.12.009
- Ghaemi, S., Li, X., Mulder, M., 2023. Economic feasibility of green hydrogen in providing flexibility to medium-voltage distribution grids in the presence of local-heat systems. August 2022 Appl. Energy 331, 120408. https://doi.org/10.1016/j. appergy.2022.120408.
- B. Golkar, R.H. Khoshkhoo, and A. Poursarvandi, "Techno-economical Comparison of MED and RO Seawater Desalination in a Large Power and Water Cogeneration Plant in Iran BT - Water Resources in Arid Areas: The Way Forward," 2017, pp. 319–333.
- Greenlee, L.F., Lawler, D.F., Freeman, B.D., Marrot, B., Moulin, P., 2009. Reverse osmosis desalination: Water sources, technology, and today's challenges. Water Res 43 (9), 2317–2348. https://doi.org/10.1016/j.watres.2009.03.010.
- Hammond, R.P., 1996. Modernizing the desalination industry. Desalination 107 (2), 101–109. https://doi.org/10.1016/S0011-9164(96)00160-9.
- Herber, G., 2024. Choosing a Desalination Plant. Medium. https://medium.com/@desalter/what-are-the-key-factors-to-consider-when-choosing-a-desalination-plant-1d1c8483606e%0A.
- Ihm, S., Al-Najdi, O.Y., Hamed, O.A., Jun, G., Chung, H., 2016. Energy cost comparison between MSF, MED and SWRO: Case studies for dual purpose plants. Desalination 397, 116–125. https://doi.org/10.1016/j.desal.2016.06.029.
- Cummins Inc., "HyLYZER WATER ELECTROLYZERS," 2021. [Online]. Available: \(\lambda\)ttps://www.cummins.com/sites/default/files/2021-08/cummins-hylyzer-250-specsheet.pdf).
- Ismail, A., 1998. Control of multi-stage flash desalination plants: A survey. Desalination 116 (2–3), 145–155. https://doi.org/10.1016/S0011-9164(98)00191-X.
- Jamaly, S., Darwish, N.N., Ahmed, I., Hasan, S.W., 2014. A short review on reverse osmosis pretreatment technologies. Desalination 354, 30–38. https://doi.org/ 10.1016/j.desal.2014.09.017.
- Jiang, S., Li, Y., Ladewig, B.P., 2017. A review of reverse osmosis membrane fouling and control strategies. Sci. Total Environ. 595, 567–583. https://doi.org/10.1016/j. scitoteny.2017.03.235.
- Jones, E., Qadir, M., van Vliet, M.T.H., Smakhtin, V., mu Kang, S., 2019. The state of desalination and brine production: A global outlook. Sci. Total Environ. 657, 1343–1356. https://doi.org/10.1016/j.scitotenv.2018.12.076.
- Joris, TikTak, 2019. Heat management for PEM electrolysis. Delft Univ.
- Kennedy, V.S., 2004. Thermal Pollution. Encycl. Energy 79–89. https://doi.org/ 10.1016/B0-12-176480-X/00416-2.
- Kesieme, U.K., Milne, N., Aral, H., Cheng, C.Y., Duke, M., 2013. Economic analysis of desalination technologies in the context of carbon pricing, and opportunities for membrane distillation. Desalination 323 (Vcd), 66–74. https://doi.org/10.1016/j. desal.2013.03.033.
- Khalilzadeh, S., Hossein Nezhad, A., 2018. Utilization of waste heat of a high-capacity wind turbine in multi effect distillation desalination: Energy, exergy and thermoeconomic analysis. Desalination 439 (October 2017), 119–137. https://doi. org/10.1016/j.desal.2018.04.010
- Khawaji, A.D., Kutubkhanah, I.K., Wie, J.M., 2008. Advances in seawater desalination technologies. Desalination 221 (1–3), 47–69. https://doi.org/10.1016/j. desal.2007.01.067
- Koninklijk Nederlands Meteorologisch Instituut (KNMI), "Dutch Offshore Wind Atlastime series files from 2008-2017 at 10-600 meter height at individual 2,5 km grid location," 2023. (https://dataplatform.knmi.nl/dataset/dowa-netcdf-ts-singlepoin t-1\)
- Liponi, A., Wieland, C., Baccioli, A., 2020. Multi-effect distillation plants for small-scale seawater desalination: thermodynamic and economic improvement. Energy Convers. Manag 205 (September 2019), 112337. https://doi.org/10.1016/j. enconman.2019.112337.
- Lüning, K., 1984. Temperature tolerance and biogeography of seaweeds: The marine algal flora of Helgoland (North Sea) as an example. Helgol. änder Meeresunters. 38 (2), 305–317. https://doi.org/10.1007/BF01997486.
- Marshall, A., Børresen, B., Hagen, G., Tsypkin, M., Tunold, R., 2007. Hydrogen production by advanced proton exchange membrane (PEM) water electrolysers-

- Reduced energy consumption by improved electrocatalysis. Energy 32 (4), 431–436. https://doi.org/10.1016/j.energy.2006.07.014.
- Mazzotti, M., Rosso, M., Beltramini, A., Morbidelli, M., 2000. Dynamic modeling of multistage flash desalination plants. Desalination 127 (3), 207–218. https://doi.org/ 10.1016/S0011-9164(00)00011-4.
- Mezher, T., Fath, H., Abbas, Z., Khaled, A., 2011. Techno-economic assessment and environmental impacts of desalination technologies. Desalination 266 (1–3), 263–273. https://doi.org/10.1016/j.desal.2010.08.035.
- Moossa, B., Trivedi, P., Saleem, H., Zaidi, S.J., 2022. Desalination in the GCC countries- a review. J. Clean. Prod. 357 (April), 131717. https://doi.org/10.1016/j. iclepro 2022.131717
- nel, "PEM Electrolyser MC Series," nel website, 2020. (https://nelhydrogen.com/product/mc-series-electrolyser/).
- Netherlands Enterprise Agency, "Offshore Wind Energy Plans 2030-2050," 2021. (https://www.rvo.nl/topics/offshore-wind-energy/plans-2030-2050).
- Plug, "The Plug EX-425D," 2024. [Online]. Available: (https://www.plugpower.com/wp-content/uploads/2022/04/EX-425D_042522.pdf).
- Prandle, D., Hydes, D.J., Jarvis, J., McManus, J., 1997. The seasonal cycles of temperature, salinity, nutrients and suspended sediment in the Southern North Sea in 1988 and 1989. Estuar. Coast. Shelf Sci. 45 (5), 669–680. https://doi.org/ 10.1006/ccss.1996.0227.
- Qasim, M., Badrelzaman, M., Darwish, N.N., Darwish, N.A., Hilal, N., 2019. Reverse osmosis desalination: A state-of-the-art review. Desalination 459 (December 2018), 59–104. https://doi.org/10.1016/j.desal.2019.02.008.
- Rahimi, B., Chua, H.T., 2017. Low. grade Heat. driven multiEff. Distill. Desalin.
- Raluy, G., Serra, L., Uche, J., 2006. Life cycle assessment of MSF, MED and RO desalination technologies. Energy 31 (13), 2361–2372. https://doi.org/10.1016/jenergy/2006.02.005
- Shiva Kumar, S., Himabindu, V., 2019. Hydrogen production by PEM water electrolysis A review. Mater. Sci. Energy Technol. 2 (3), 442–454. https://doi.org/10.1016/j. mset.2019.03.002.
- Siachos, K., 2022. Offshore Green. Hydrog. Prod. Transp. shore via Pipelines North Sea Parallel Nat. Gas. Transp.
- Sola, I., et al., 2020. Sustainable desalination: Long-term monitoring of brine discharge in the marine environment. Mar. Pollut. Bull. 161 (September). https://doi.org/ 10.1016/j.marpolbul.2020.111813.
- A. Steinbach, "Advanced Manufacturing Processes for Gigawatt-Scale Proton Exchange Membrane Water Electrolyzers," 2023. [Online]. Available: (https://www.hydrogen.energy.gov/docs/hydrogenprogramlibraries/pdfs/review23/p197_steinbach_2023_0-pdf.pdf?sfvrsn=3d8f44_0).
- Swertz, O.C., Colijn, F., Hofstraat, H.W., Althuls, B.A., 1999. Temperature, salinity, and fluorescence in Southern North Sea: High- resolution data sampled from a ferry. Environ. Manag. 23 (4), 527–538. https://doi.org/10.1007/s002679900207.
- Swiss, Aqua, 2024. Comp. Sel. Desalin. Process. (http://aquaswiss.eu/wp-content/uploads/2016/03/medysro.pdf).
- The Government of Netherlands, "Climate Agreement," The Hague, Jun. 2019. [Online].

 Available: \(\lambda \text{ttps://www.government.nl/binaries/government/documenten/report \)

 \$\(\frac{2019}{6} \frac{28}{c} \text{limate-agreement/Climate-Agreement.pdf} \).
- D. Thomas, "Large scale PEM electrolysis: technology status and upscaling strategies," 2019. [Online]. Available: http://hybalance.eu/wp-content/uploads/2019/10/ Large-scale-PEM-electrolysis.pdf.
- Van der Welle, A.J., De Joode, J., 2011. Regulatory road maps for the integration of intermittent electricity generation: Methodology development and the case of The Netherlands. Energy Policy 39 (10), 5829–5839. https://doi.org/10.1016/j. enpol_2011_06_017
- Veolia, "Distillation Processes for Sea Water Desalination The technology Multiple Effect Distillation with Mechanical Vapour Compression (MED-MVC)," 2014. [Online]. Available: http://www.veoliawatertech.com/nawatersytems/ressources/documents/1/20581,MultiEffectDistillation.pdf).
- Villagra, A., Millet, P., 2019. An analysis of PEM water electrolysis cells operating at elevated current densities. Int. J. Hydrog. Energy 44 (20), 9708–9717. https://doi. org/10.1016/j.ijhydene.2018.11.179.
- Voutchkov, N., 2012. Desalin. Eng. Plan. Des. McGraw Hill 2012.
- Wang, X., Christ, A., Regenauer-Lieb, K., Hooman, K., Chua, H.T., 2011. Low grade heat driven multi-effect distillation technology. Int. J. Heat. Mass Transf. 54 (25–26), 5497–5503. https://doi.org/10.1016/j.ijheatmasstransfer.2011.07.041.
- Wenten, I.G., Khoiruddin, 2016. Reverse osmosis applications: Prospect and challenges. Desalination 391, 112–125. https://doi.org/10.1016/j.desal.2015.12.011.
- Zhao, D., Xue, J., Li, S., Sun, H., Zhang, Q. dong, 2011. Theoretical analyses of thermal and economical aspects of multi-effect distillation desalination dealing with highsalinity wastewater. Desalination 273 (2–3), 292–298. https://doi.org/10.1016/j. desal.2011.01.048.